Research Article

Synthesis, characterization and evaluations of micro/mesoporous ZSM-5 zeolite using starch as bio template

R. Sabarish[1] · G. Unnikrishnan[1]

Abstract

We report a simple and economical method to synthesis hierarchical ZSM-5 zeolite using a natural polymer, soluble starch, as a mesotemplate. The synthesized samples were characterized with X-ray diffraction, Fourier transform infrared spectroscopy, field emission scanning electron microscopy, transmission electron microscopy, nitrogen sorption, ammonia temperature-programmed desorption and thermogravimetric analysis. The crystallinity and Mordenite Framework Inverted structure of the samples was confirmed by X-ray diffraction and Fourier transform infrared spectroscopy analysis. Scanning electron microscopy and transmission electron microscopy images revealed the presence of mesopores in the synthesized samples. The nitrogen adsorption/desorption results of the hierarchical samples have been found to be in agreement with the scanning electron microscopy and transmission electron microscopy results and support the development of mesoporosity. The acidity of the hierarchical zeolite was studied using ammonia temperature-programmed desorption. The thermogravimetric analysis confirmed the thermal stability of the synthesized samples up to 750 °C. The catalytic activities of the modified and unmodified zeolites were specifically tested for the esterification of acetic acid with benzyl alcohol. The results indicate that the hierarchical ZSM-5 catalyst offers a better catalytic yield (76%) than the unmodified systems.

✉ G. Unnikrishnan, unnig@nitc.ac.in; R. Sabarish, sabarishchem@gmail.com | [1]Department of Chemistry, National Institute of Technology, Calicut, Kerala 673601, India.
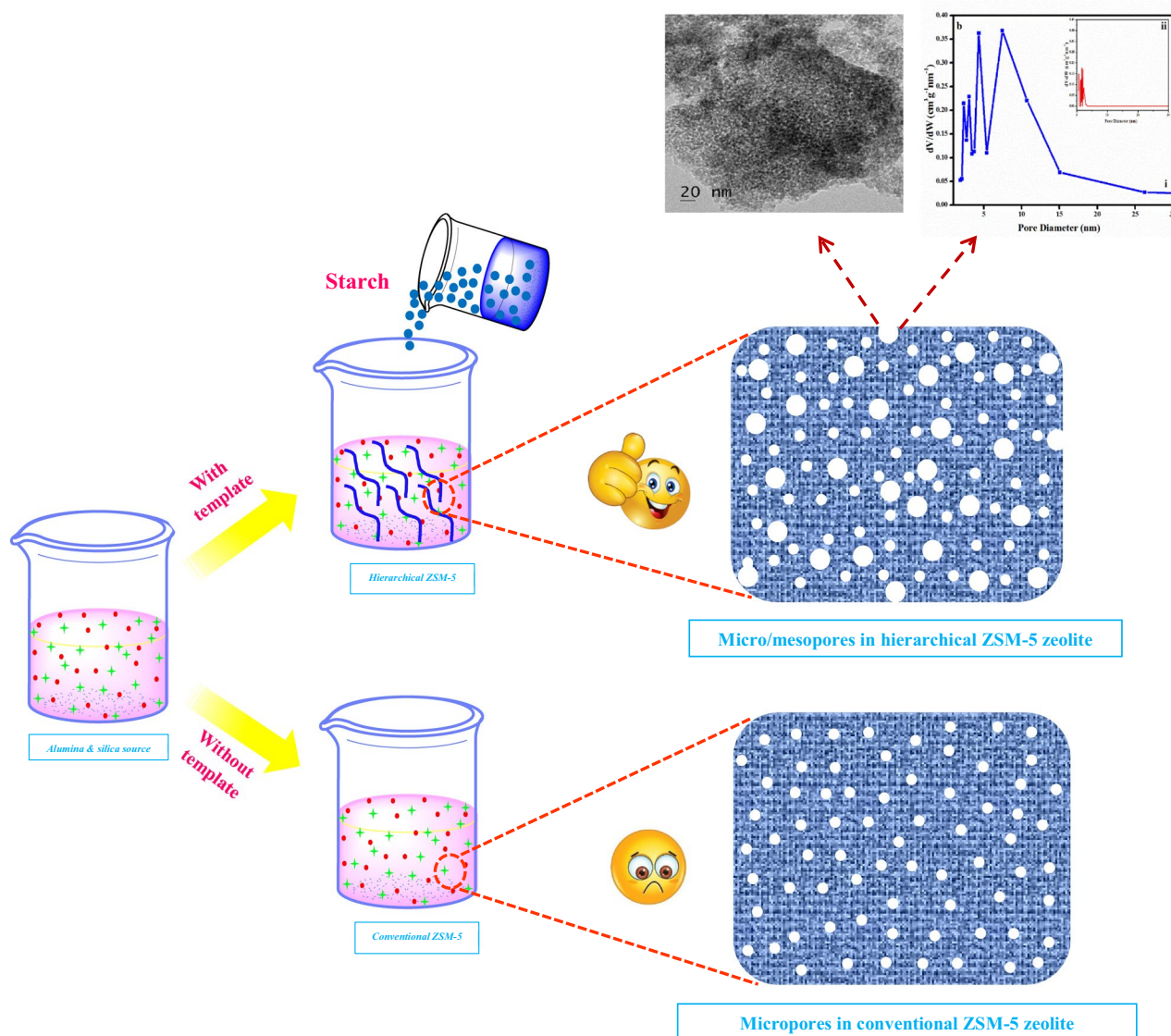
Graphic abstract

Keywords Hierarchical zeolite · Mesoporous · Starch template · Catalytic activity

1 Introduction

Zeolites are naturally occurring aluminosilicates with crystalline microporous structure [1, 2]. The unique structure of zeolites is responsible for their interesting applications in catalysis, adsorption, water purification etc. [3–5]. The outstanding ability of zeolites to catalyse petrochemical processes such as cracking, isomerization, aromatization and alkylation process inspire scientists to explore their further catalytic applications [6–9]. One of the drawbacks of zeolites is the small pores within them, which significantly limits the diffusion of large molecules through them and

hence the inability to catalyse large molecular reactions [10]. Fabrication of zeolites with meso/macroporous is an ideal strategy to address this issue. The enhanced surface area and porosity of hierarchical zeolites assist them to exhibit improved catalytic performance than conventional zeolites [11, 12].

Different strategies were employed to tune the pore sizes of zeolites [13, 14]. Templating method, which utilizes different templating agents such as carbon black, surfactants, polymers, polystyrene bead, tetrapropylammonium (TPA^{+}) ions etc. is one of the widely used techniques to synthesis hierarchical zeolites [15–20]. A number

of reports are available in literature on template-assisted synthesis of hierarchical zeolites. Jacobsen et al. [21] successfully synthesized a mesoporous zeolite using carbon template and observed higher catalytic performance for large molecular reactions. Narayanan et al. [22] recently developed a hierarchical zeolite using a soft surfactant template (Triton X100).

Tailoring hierarchical zeolites with naturally occurring templating agents such as chitosan, agricultural wastes, cellulose, starch etc. is reported in literature. Krishnan and co-workers developed hierarchical ZSM-5 monolith using corn and sorghum stem pith as templates [23]. Jin et al. [24] successfully synthesized mesoporous zeolite using ammonium-modified chitosan as template and demonstrated its high catalytic activity for Claisen–Schmidt condensation. A few attempts have been made in the past to use starch as template to introduce mesoporosity in zeolite. Wang et al. [25] successfully fabricated different types of zeolites (silicalite-1, ZSM-5, TS-1) using soluble starch and carboxymethyl cellulose as templates using basic medium NaOH. A facial route to synthesize mesoporous hierarchical zeolites using starch derived bread as a template was reported by Xiao et al. [26]. Recently, Zhang et al. [27] synthesized ZSM-5 zeolite with intracrystal mesopores using soluble starch as an in situ template.

Esterification of carboxylic acids with alcohols using homogeneous and heterogeneous catalysts have been the subject of investigation by many workers [28, 29]. Generally, the synthesis of esters requires the use of mineral acids, which are toxic and hazardous. Researchers are currently focussing to develop more environmental-friendly methods for the production of esters. It is a well-established fact that the zeolites are efficient acid heterogeneous catalysts for several organic reactions [30–32]. Attempts are being done, with great enthusiasm, to enhance their catalytic activity through different routes. In this work, hierarchical zeolites have been developed from ZSM-5, using starch mesotemplate. The efficiency of the modified zeolite has been tested for the esterification of acetic acid with benzyl alcohol.

2 Experimental

2.1 Chemicals

Tetrapropyl ammonium hydroxide ($(CH_3CH_2CH_2)_4NOH$; TPAOH), tetraethyl orthosilicate ($C_8H_{20}O_4Si$; TEOS) and aluminum isopropoxide ($C_9H_{21}AlO_3$; AIP) were purchased from Sigma Aldrich Co. Ltd (India). Acetic acid (CH_3COOH), benzyl alcohol ($C_6H_5CH_2OH$) and soluble starch ($C_6H_{10}O_5)_n$ used were of reagent grade, procured from Merck, and used without further purification.

2.2 Synthesis

The hierarchical ZSM-5 zeolite was synthesized by a hydrothermal crystallization route. In a typical synthesis, 0.03 g of aluminum isopropoxide (AIP) and 2.11 g of tetrapropylammonium hydroxide (TPAOH) were mixed to obtain a clear solution. 3.46 g of tetraethyl orthosilicate (TEOS) and 7 g of distilled water were added to it under constant stirring for 5–6 h. To the resulting solution, 0.2 g of starch was added under constant stirring. It was then concentrated at 80 °C in a rotavapor for 20 min to get a transparent sticky solution. It was transferred into an autoclave, and kept at 80 °C for 24 h. The sample was later hydrothermally treated at 175 °C for 6 h. The obtained product was washed with deionized water, dried in air, and calcined at 550 °C for 5 h to remove the organic components. The hierarchical zeolite so obtained has been designated as ZSM-5 WS. For comparison, another sample using the same procedure but without the template i.e. ZSM-5 WOS was also synthesized.

2.3 Catalytic reaction

2.3.1 Esterification of acetic acid with benzyl alcohol

Catalytic activity studies of esterification of acetic acid with benzyl alcohol was carried out in two-neck round bottom flask connected with reflux condenser, a thermometer and magnetic stirrer. In a typical run, the catalyst 0.09 g was mixed with 20 mmol of benzyl alcohol and 5 mmol of acetic acid were carried out at 110 °C at 3 h under constant magnetic stirring. Finally, the reaction mixture was centrifuged, filtered and analyzed through GC with an FID
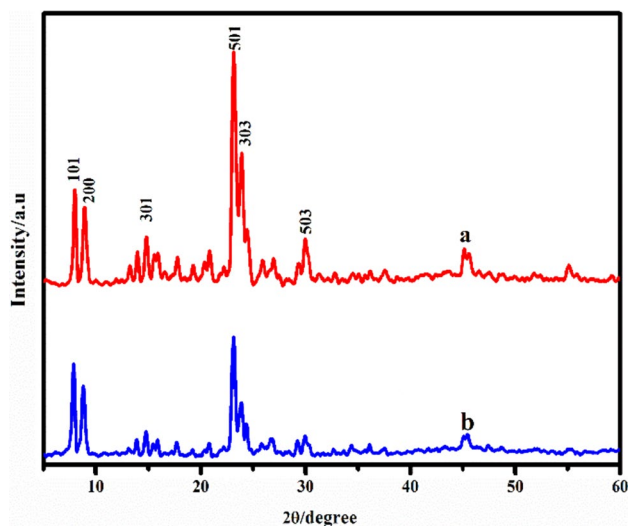

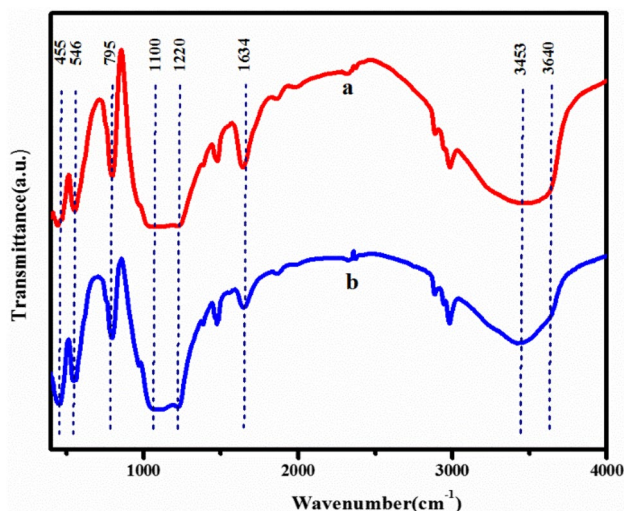**Fig. 1** XRD patterns of: (a) ZSM-5 WOS and (b) ZSM-5 WS

Fig. 2 FTIR spectra of: (a) ZSM-5 WOS and (b) ZSM-5 WS

detector and an Rtx@5 column. Nitrogen was used as the carrier gas.

2.4 Characterization

X-ray diffraction (XRD) patterns were obtained with a Rigaku Miniflex 2200 diffractometer using CuKα radiation. Scanning electron microscopic images were obtained by using a Hitachi SU6600 Variable Pressure Field Emission Scanning Electron Microscope (SEM). FT-IR spectrum was recorded at room temperature using an FT-IR spectrometer Jasco 4700 in the range of 400–4000 cm^{-1}. Thermogravimetric (TG) analysis of the uncalcined zeolite samples

(TG) was done using a TGA Instrument Q50 at a heating rate of 10 °C/min in nitrogen. BET surface area and pore size distributions were measured by N$_2$ adsorption–desorption using a Micromeritics Gemini V-2380 surface area analyzer. NMR spectra were recorded on a Bruker Avance AV 300 spectrometer. Transmission electron microscopic images (TEM) were obtained with a JEOL JEM-2100 transmission electron microscope operated at an accelerating voltage of 200 kV. The temperature programmed desorption (TPD) patterns with ammonia on the samples were recorded on Micromeritics Chemisorb 2750.

3 Result and discussion

3.1 XRD

XRD patterns of the modified and unmodified ZSM-5 zeolite samples are shown in Fig. 1. The appearance of characteristic MFI peaks at 2θ = 8.0, 9.0, 14.8, 22.9, 24.0 and 29.8 is attributed to the 101, 200, 301, 501, 303 and 503 crystalline nature of the synthesized sample (JCPDS no. 42-0024) [33–35]. It can be noted that the intensity of crystalline peak is slightly reduced in modified ZSM-5 zeolite (Fig. 1b) attributed to the generation of disordered mesopores or due to the some of the mesoporous walls are not converted into MFI structure [15, 22, 36].

3.2 FT-IR

In order to confirm the MFI structure of the samples, the FT-IR analysis was done and the spectra are depicted in
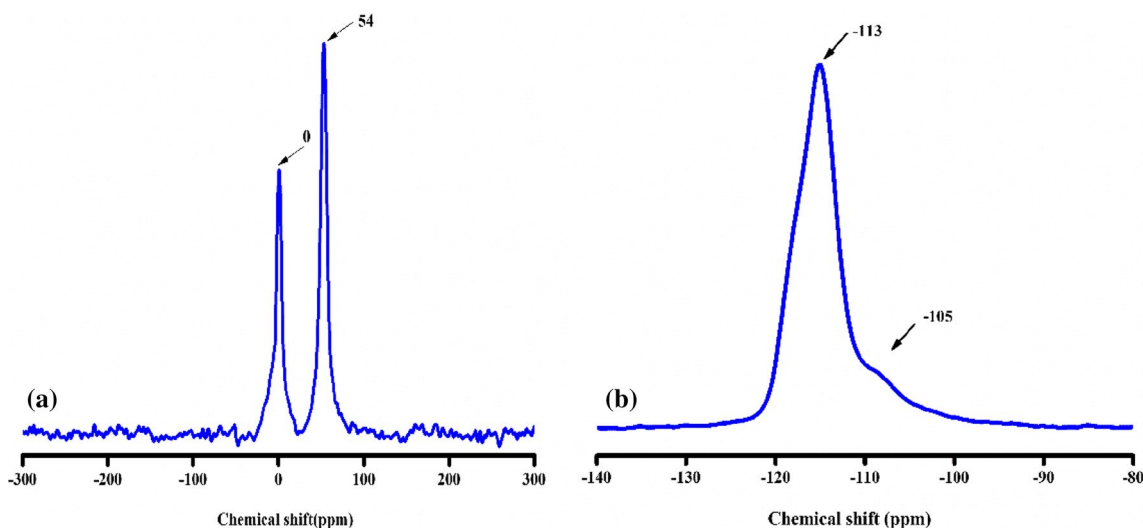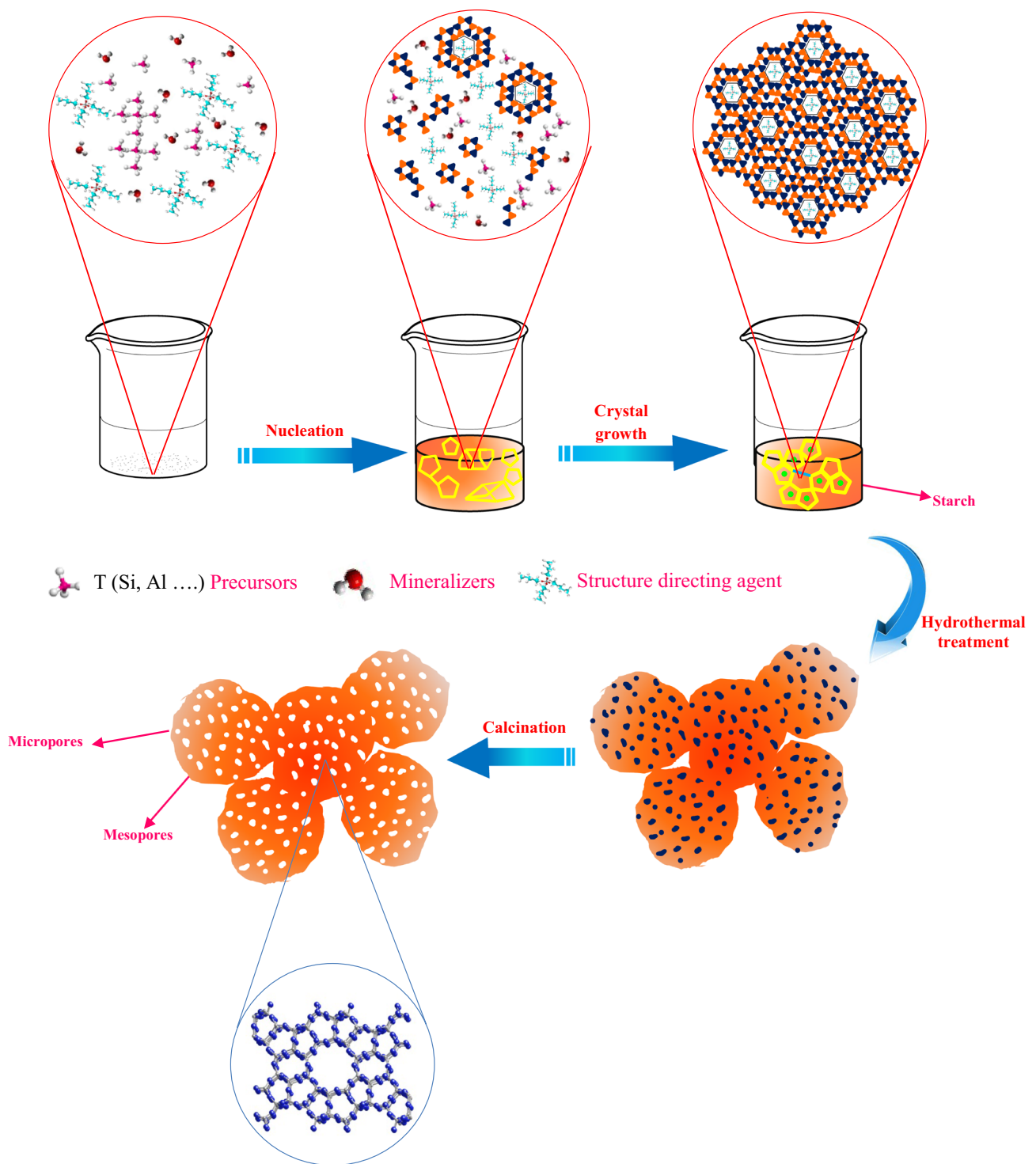

Fig. 3 **a** ^{27}Al and **b** ^{29}Si NMR spectra of ZSM-5 WS

Scheme 1 Formation of micro/mesoporous in ZSM-5

Fig. 2a, b. FT-IR spectra of both modified and unmodified samples show absorption bands at 1224 cm^{-1} (external asymmetric stretch), 1150–1050 cm^{-1} (internal asymmetric stretch), 795 cm^{-1} (external symmetric stretch) and at 445 cm^{-1} (T–O bend). The peak at 3640 cm^{-1} is attributed to the isolated silanol groups (Si–O–H) while the peak at 3453 cm^{-1} corresponds to the Al–OH framework (Brønsted acid sites). The band observed at 546 cm^{-1} is assigned to the double-5 ring of crystalline ZSM-5 [37, 38]. This further
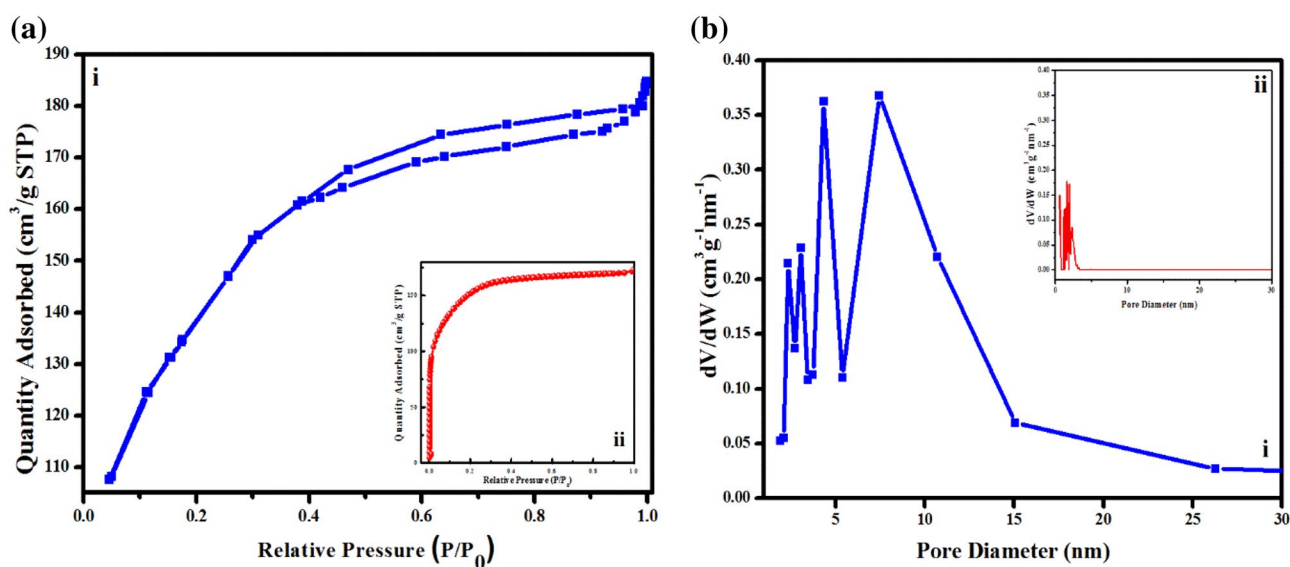
(a)

(b)

Fig. 4 **a** N$_2$ adsorption isotherms of (i) ZSM-5 WS, (ii) (inset) ZSM-5 WOS; **b** pore size distribution of: (i) ZSM-5 WS (ii) (inset) ZSM-5 WOS

confirms that both the modified and unmodified samples have the characteristic MFI structure.

3.3 Al and Si MAS NMR

^{27}Al MAS and ^{29}Si NMR spectra for the modified ZSM-5 zeolites are shown in Fig. 3. The ^{27}Al MAS NMR analysis exhibit a two signal at ~ 0 ppm and ~ 54 ppm confirming that the Al species are octahedral and tetrahedral coordinated in the framework of the mesoporous ZSM-5 zeolite. The large intense peak observed at ~ 54 ppm corresponds to the tetrahedral Al co-ordination in the framework while the low-intensity peak, centered at ~ 0 ppm, is due to octahedral Al. Meanwhile, the Si NMR spectra of the sample show a major peak at ~ 113 ppm, corresponding to Si (4Si) (Q)^4 and a weak shoulder peak at ~ 105 ppm due to Si (3Si, 1 Al) or Si (3Si, 1 OH) respectively [39].

A representation for the development of micro and meso dimensions in zeolite is shown in Scheme 1. Initially, the silicate and aluminate combine together to form an amorphous aluminosilicate gel with Si–O–Si and Si–O–Al bonds. Meso and micro-templates, then, organize around the developed SiO$_4$ and AlO$_4$ tetrahedral units, and induce the formation of specific types of pores/channels in the zeolite structure. The hydrothermal treatment and aging, subsequently, convert the amorphous aluminosilicate into crystalline zeolite. Finally, upon calcination, micro/mesotemplates are removed to generate micro and meso dimensions in zeolite.

3.4 N$_2$ isotherm

The porosity of the samples was analyzed using N$_2$ adsorption method. The N$_2$ adsorption/desorption isotherms of the samples are shown in Fig. 4a. It can be noted that the modified sample exhibits type IV adsorption peak, whereas the unmodified zeolite displays type I curve. The modified sample shows a major uptake at a relative pressure P/P$_o$ > 0.4 indicating the presence of mesopores (Fig. 4b). Furthermore, the Barrett-Joyner-Halenda (BJH) pore-size distribution was found to be in the range of 5–15 nm confirming the presence of mesopores in the system.

3.5 SEM and TEM

Scanning electron microscopy (SEM) and transmission electron microscopy (TEM) images provide detailed information about the morphology and structure of the samples. Figure 5a, b show the SEM images of unmodified and modified samples respectively. As can be seen from Fig. 5b the surface of the sample is rough with non-uniform distribution of particles. The presence of mesopores is clearly visible in the SEM image of the modified sample. The TEM images of the modified ZSM-5 zeolite sample demonstrate zeolite nanocrystals with many bright areas, indicating the presence of mesopores [24, 27]. These results were complementary to BET and SEM analysis and support the successful generation of mesopores in the modified sample. The selected area diffraction (SAED) pattern is shown in the inset of Fig. 6d. Development of a well-defined 2D lattice fringes, reveals that the zeolite particles possess
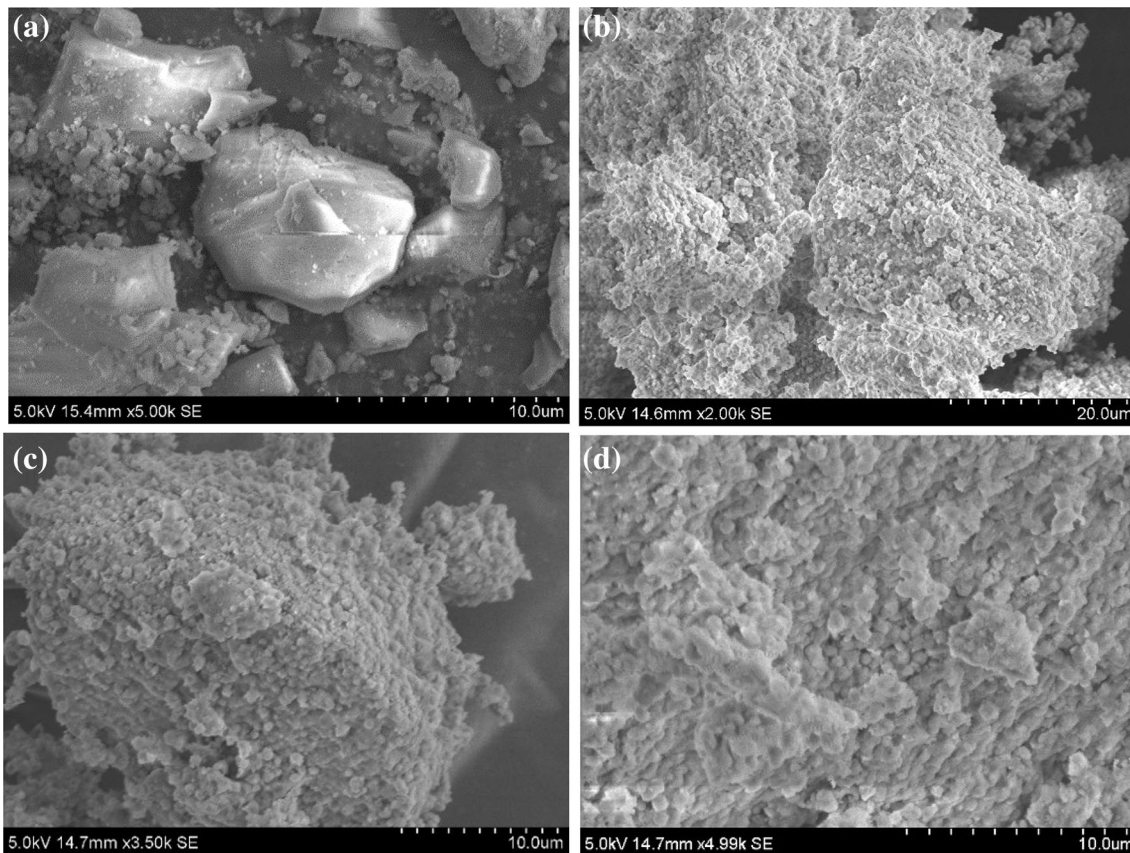
Fig. 5 SEM images of **a** ZSM-5 WOS, **b**–**d** ZSM-5 WS with three magnifications

significant crystallinity even after modification with the starch template.

3.6 Acidity

The acidity of the ZSM-5 WS and ZSM-5 WOS was evaluated using ammonium TPD analysis and the profile is presented in Fig. 7. It is evident that both the samples show two desorption peaks which is in good agreement with the previous literature [40]. The peak at low temperature is attributed to the desorption of physisorbed ammonia by weak acid sites while the peak at high temperature is due to the desorption of ammonia from strong acidic sites, such as Brønsted acidic sites [41]. However, the acidity of ZSM-5 WS is found to be slightly lower than ZSM-5 WOS which is attributed due to the presence of mesopores in the former [42–44].

3.7 TG/DTG

The results of the thermogravimetric analysis of ZSM-5 WOS and ZSM-5 WS are given in Fig. 8. The TG of both unmodified and modified ZSM-5 catalyst displayed an initial weight loss at 100 °C due to the removal of physically adsorbed water molecules from the surface of the sample. The second weight loss in the range of 400–500 °C could be due to the decomposition of structure directing agent TPAOH. In the case of modified ZSM-5 zeolite a third weight loss at 300 °C is also observed, attributed to the removal of excess unreacted starch. Accordingly, three peaks at 150, 300 and 550 °C have been noted in DTG.

3.8 Esterification of acetic acid with benzyl alcohol

Esterification of acetic acid with benzyl alcohol is being thoroughly examined by researchers worldwide as the obtained product, benzyl acetate, has significant industrial importance for the manufacture of paints, varnishes and perfumes etc. [45, 46]. This reaction is selected as the model reaction in this work to test the catalytic activity of the modified sample. The effects of parameters such as molar ratio of the reactants, catalyst quantity, reaction temperature and time on reaction kinetics have been investigated.

A comparison of percentage conversion of benzyl alcohol without catalyst, with unmodified (WOS) and
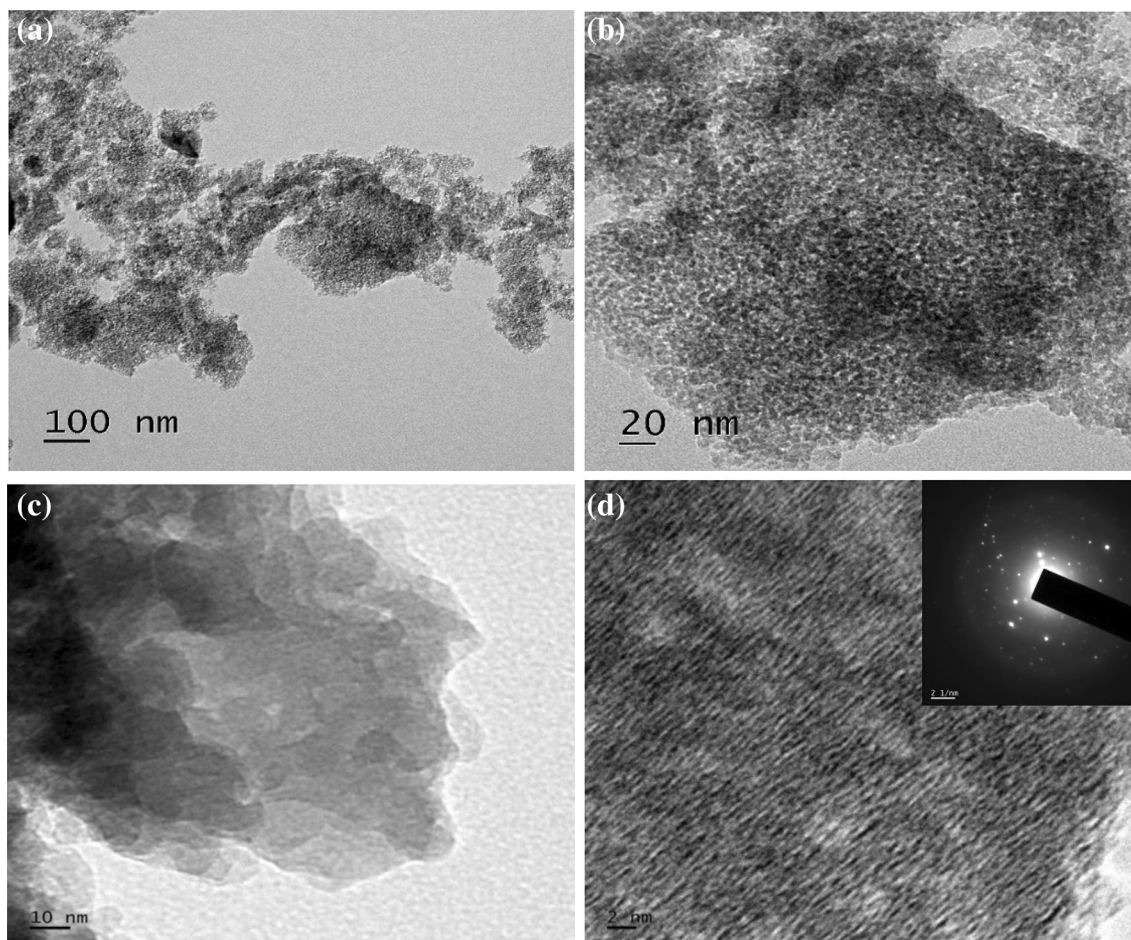
Fig. 6 TEM images of ZSM-5 WS **a**–**d** with different magnification
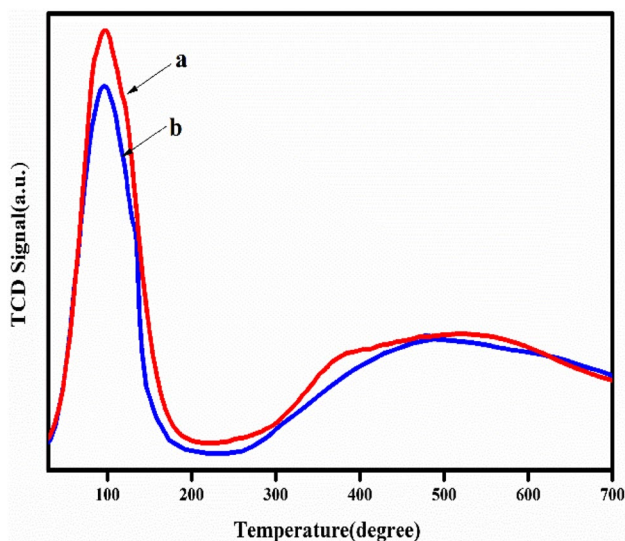

Fig. 7 NH$_3$-TPD profiles of (a) ZSM-5 WS (b) ZSM-5 WOS

modified catalyst (WS) catalyst is shown in Fig. 9a. It is evident that the hierarchical zeolite executes a higher benzyl alcohol conversion than other two catalysts. The WOS catalyst displays 100% selectivity for benzyl acetate because the small micropores in it will hinder the transport of larger molecule, dibenzyl ether. However, the presence of large mesoporous in WS catalyst, facilitate the formation of dibenzyl ether and consequently, we can observe a slight decrease in selectivity for benzyl acetate. Initially, the effect of molar ratio of reactants on the conversion and selectivity to benzyl acetate was studied by varying the molar ratio of acetic acid to alcohol from 1:1 to 1:5 (Fig. 9b). On increasing the molar ratio of AA: BA from 1:1 to 1:4, the conversion of benzyl alcohol increase from 53 to 76%. Above 1:4 molar ratio, only a slight increase in conversion was observed and therefore all further reaction was performed with a molar ratio of 1:4. With increase in molar ratio, the selectivity of benzyl acetate decreases from 96 to 93% and selectivity of dibenzyl ether increases
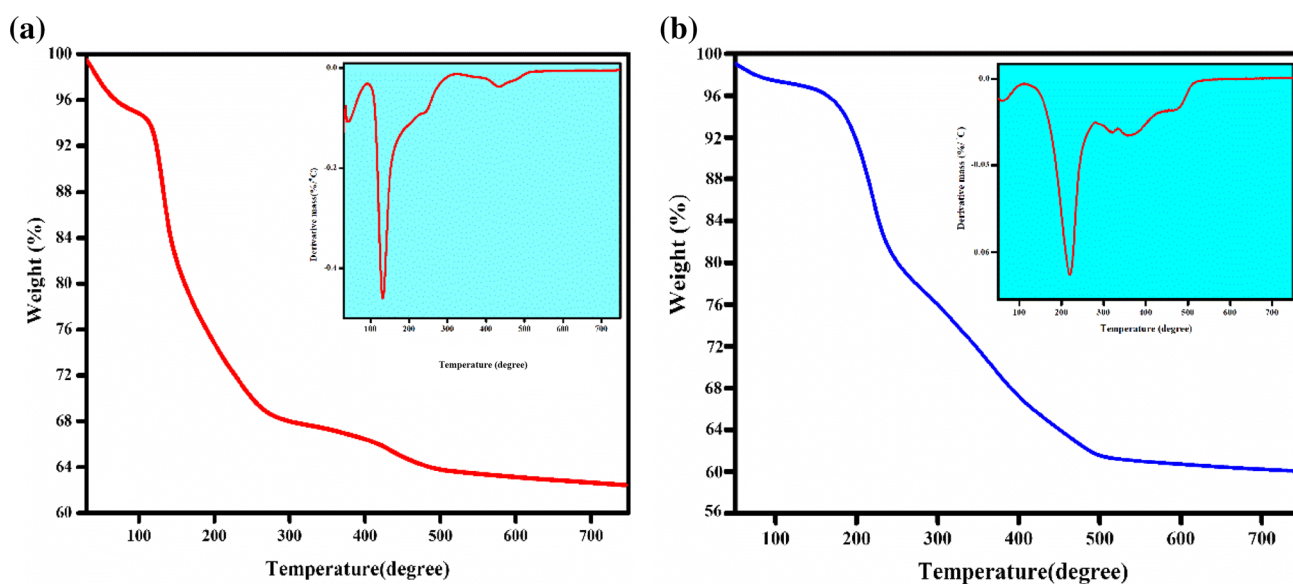
Fig. 8 TG curve of: **a** ZSM-5 WOS and **b** ZSM-5 WS (DTG curves are given at the inset)
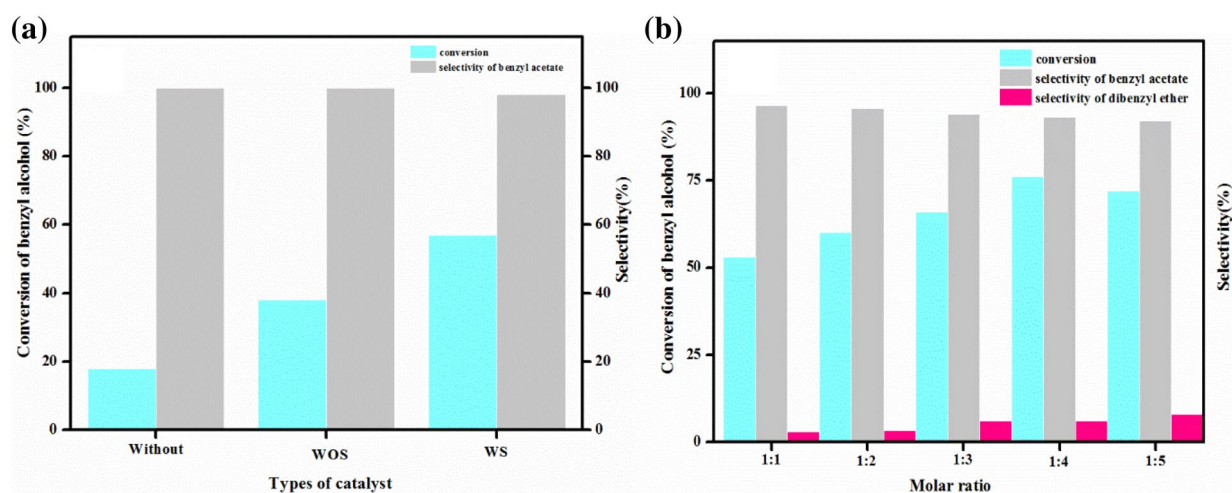

Fig. 9 Effect of: **a** different catalyst; **b** molar ratio on the esterification of acetic acid with benzyl alcohol: Experimental conditions: benzyl alcohol: acetic acid—4:1, catalyst—0.09 g, time-3 h, temperature—110 °C

from 3 to 6%. This is attributed to the presence of micro/mesoporous structure which will facilitate the formation of dibenzyl ether. We propose a multi-layer mechanism for this reaction with modified zeolite, as shown in Scheme 2.

The effect of catalyst amount on the reaction was evaluated by varying the catalyst from 0.03 to 0.12 g, while keeping the molar ratio of AA: BA at 1:4. As expected the benzyl alcohol conversion increases with an increase in catalyst amount. Further increase in catalyst content shows a decrease in benzyl alcohol conversion. It is evident from Fig. 10a that the amount of catalyst affects the selectivity of the product. On increasing the catalyst loading from 0.03 to 0.12, the selectivity of benzyl acetate

decreases from 96 to 87%, while the selectivity of dibenzyl ether increase from 4 to 13. Therefore 0.09 g catalyst with 76% conversion and 93% selectivity for benzyl acetate was selected as optimized catalyst concentration. In the present work, esterification reaction was carried out in the temperature range of 100–130 °C while keeping the acid: alcohol molar ratio at 1:4 and the catalyst weight at 0.09 g. It can be seen from Fig. 10b that with an increase in temperature, the conversion of benzyl alcohol increases from 63 to 87% while the selectivity for benzyl acetate was found to be decreased slightly at high temperature. This is attributed to the formation of dibenzyl ether formation at high temperature.
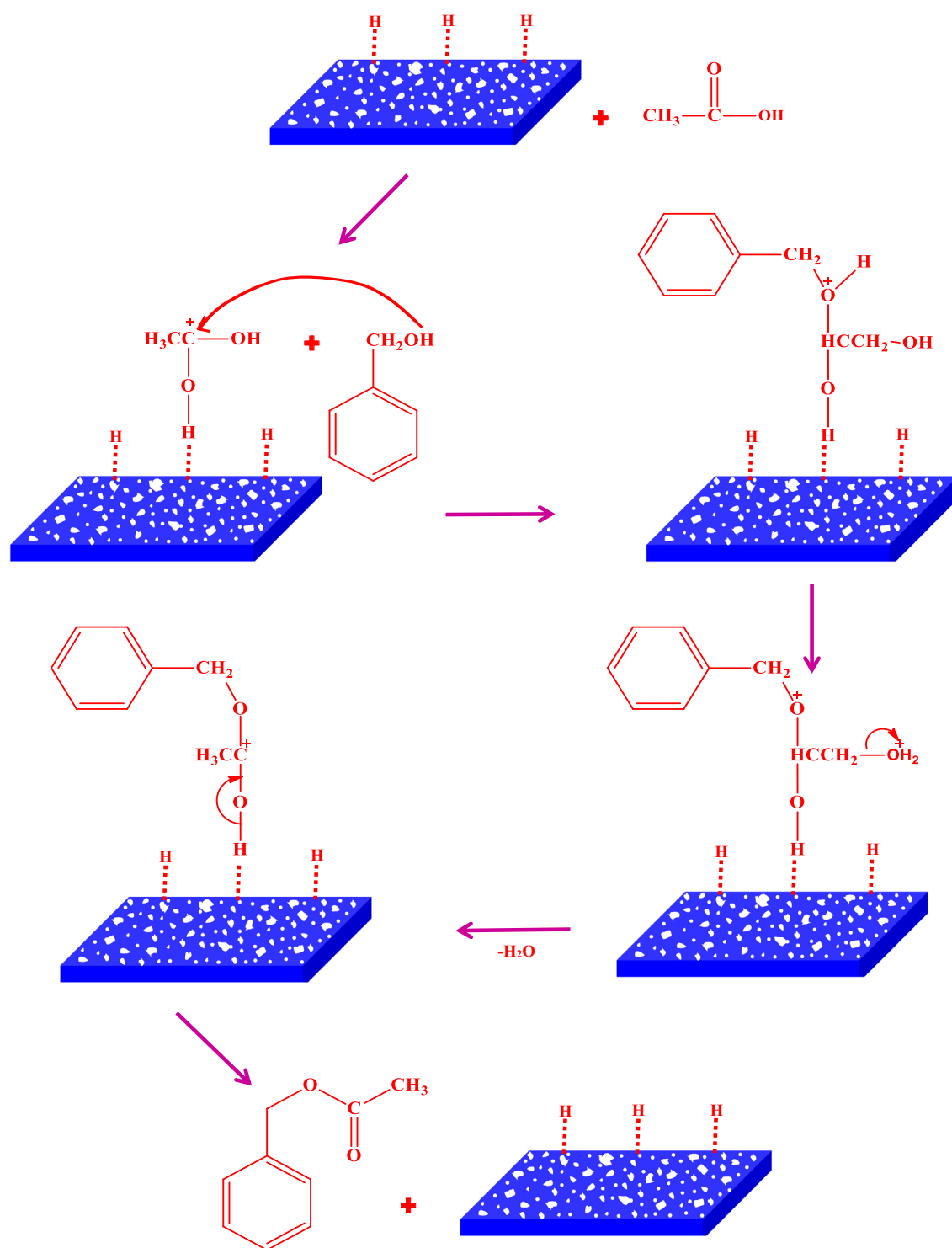
Scheme 2 Mechanism of ester hydrolysis on zeolite surface

The study was further extended to optimize the reaction time, with acid: alcohol molar ratio at 1:4 and catalyst concentration at 0.09 g. The results are presented in Fig. 11a. The benzyl alcohol conversion for WS has been observed to be increased from 58 to 78% with an increase in reaction time up to 3 h. After 3 h, only a slight increase in benzyl alcohol conversion was observed with a slight reduction in benzyl acetate selectivity. For industrial application, the reusability of the catalyst is very important. Therefore, the reusability of the catalysts for
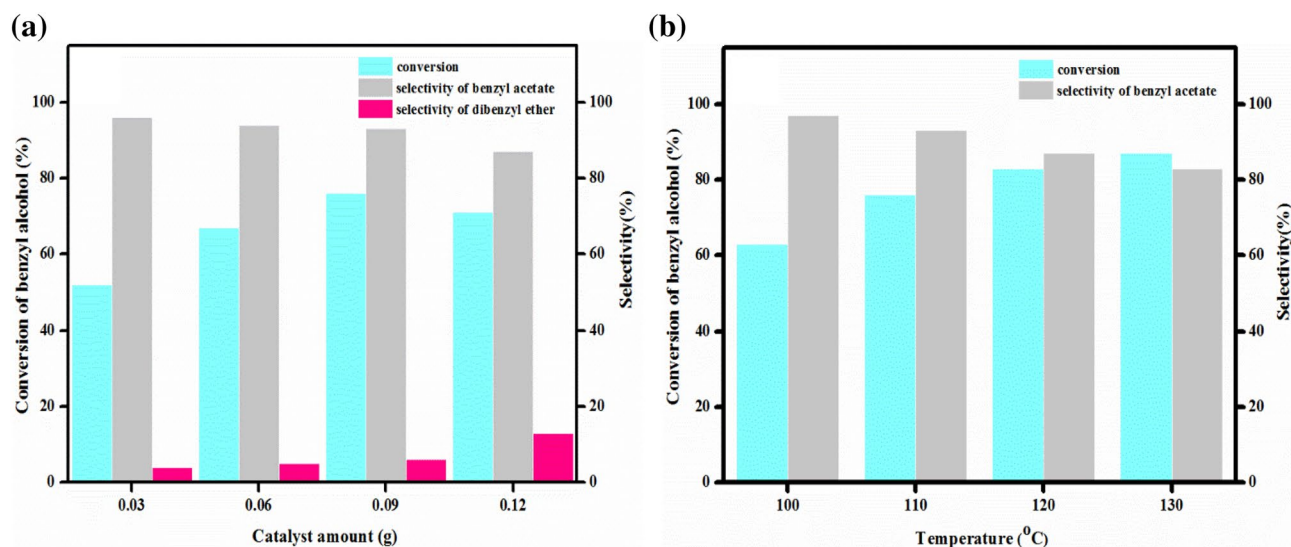
(a)

(b)

Fig. 10 Effect of: **a** catalyst amount; **b** temperature on the esterification of acetic acid with benzyl alcohol: experimental conditions: benzyl alcohol: acetic acid—4:1, catalyst—0.09 g, time-3 h, temperature—110 °C

(a)

(b)

Fig. 11 Effect of: **a** time; **b** reusability on the esterification of acetic acid with benzyl alcohol: experimental conditions: benzyl alcohol: acetic acid—4:1, catalyst—0.09 g, time-3 h, temperature—110 °C
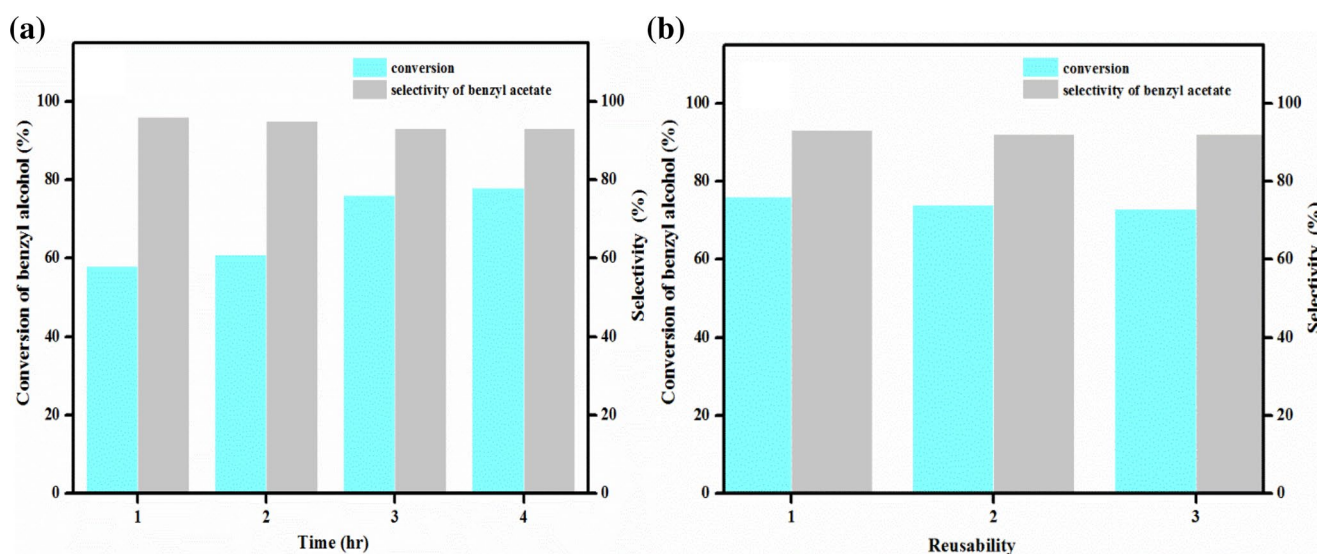
the esterification of acetic acid with benzyl alcohol was examined. The catalyst has been found to be reusable at least three times with washing with water and subsequent drying after every cycle of operation (Fig. 11b).

4 Conclusions

Fabrication of hierarchical ZSM-5 zeolite was successfully achieved by using an environment -friendly mesotemplate, starch. The synthesized ZSM-5 exhibited good crystallinity, high surface area, high porosity and thermal stability, making it an ideal candidate in the field of catalysis and adsorption. The modified ZSM-5 catalyst showed better catalytic activity for esterification reaction than the unmodified ZSM-5 catalyst.

Compliance with ethical standards

Conflict of interest The authors declare no conflict of interest.

References

1. Bekkum HV, Flanigen EM, Jacobs PA, Jansen JC (2001) Studies in surface science and catalysis, Introduction to zeolite science and practice. Elsevier, Amsterdam, p 137
2. Dyer A (1988) An introduction to zeolite molecular sieves. Wiley, New York. https://doi.org/10.1002/sia.740140410
3. Corma A (1997) From microporous to mesoporous molecular sieve materials and their use in catalysis. Chem Rev 97:2373–2419. https://doi.org/10.1021/cr960406n
4. Ozin GA, Kuperman A, Stein A (1989) Advanced zeolite, materials science. Angew Chem Int Ed 28:359. https://doi.org/10.1002/anie.198903591
5. Egeblad K, Christensen CH, Kustova M, Christensen CH (2008) Templating mesoporous zeolites. Chem Mater 20:946–960. https://doi.org/10.1021/cm702224p
6. Clerici MG (2000) Zeolites for fine chemicals production. Top Catal 13:373–386. https://doi.org/10.1023/a:1009063106954
7. Kim J, Choi M, Ryoo R (2010) Effect of mesoporosity against the deactivation of MFI zeolite catalyst during the methanol-to-hydrocarbon conversion process. J Catal 269:219–228. https://doi.org/10.1016/j.jcat.2009.11.009
8. Zhao XB, Guo XW, Wang XS (2006) Characterization of modified nanoscale ZSM-5 catalyst and its application in FCC gasoline upgrading process. Energy Fuels 20:1388–1391. https://doi.org/10.1021/ef060004a
9. Choudhary VR, Kinage AK, Choudhary TV (1997) Low-temperature nonoxidative activation of methane over *H*-Galloaluminosilicate (MFI) zeolite. Science 275:1286–1288. https://doi.org/10.1126/science.275.5304.1286
10. Bjørge M, Joensen F, Holm SM, Olsbye U, Lillerud KP, Svelle S (2008) Methanol to gasoline over zeolite H-ZSM-5: improved catalyst performance by treatment with NaOH. Appl Catal A 345:43–50. https://doi.org/10.1016/j.apcata.2008.04.020
11. Groen JC, Peffer LAA, Moulijn JA, Ramírez JP (2004) On the introduction of intracrystalline mesoporosity in zeolites upon desilication in alkaline medium. Microporous Mesoporous Mater 69:29–34. https://doi.org/10.1016/j.micromeso.2004.01.002
12. Hartmann M (2004) Hierarchical zeolites: a proven strategy to combine shape selectivity with efficient mass transport. Angew Chem Int Ed 43:5880–5882. https://doi.org/10.1002/anie.200460644
13. Seifert J, Emig G (1987) Studies of the microstructure of porous solids by physisorption measurements. Chem Ing Tech 59:475–484. https://doi.org/10.1002/cite.330590606
14. Maier WF, Tilgner IC, Wiedorn M, Ko HC (1993) Preparation and characterization of microporous metal oxides. Adv Mater 5:726–730. https://doi.org/10.1002/adma.19930051008
15. Han S, Wang Z, Meng L, Jiang N (2016) Synthesis of uniform mesoporous ZSM-5 using hydrophilic carbon as a hard template. Mater Chem Phys 177:112–117. https://doi.org/10.1002/adma.19930051008
16. Jin L, Xie T, Liu S, Li Y, Hu H (2016) Controllable synthesis of chainlike hierarchical ZSM-5 templated by sucrose and its catalytic performance. Catal Commun 75:32–36. https://doi.org/10.1016/j.catcom.2015.12.002
17. Mirzababaei SN, Taghizadeh M, Alizadeh M (2016) Synthesis of surfactant-modified ZSM-5 nanozeolite for the removal of nickel (II) from aqueous solution. Desalin Water Treat 57:12204–12215. https://doi.org/10.1080/19443994.2015.1049556
18. Zhang Y, Zhu K, Duan X, Zhou X, Yuan WJ (2014) Templating effect of an easily available cationic polymer with widely separated charge centers on the synthesis of hierarchical ZSM-5 zeolite. Mater Chem A 2:18666–18676. https://doi.org/10.1039/c4ta02325k
19. Parkhomchuk EV, Semeykina VS, Sashkina KA, Okunev AG, Lysikov AI, Parmon VN (2016) Synthesis of polystyrene beads for hard-templating of three-dimensionally ordered macroporosity and hierarchical texture of adsorbents and catalysts. Top Catal 60:178–189. https://doi.org/10.1007/s11244-016-0719-3
20. Parkhomchuk EV, Sashkina KA, Rudina NA, Kulikovskaya NA, Parmon VN (2013) Template synthesis of 3D-structured macroporous oxides and hierarchical zeolites. Catal Ind 5:80–89. https://doi.org/10.1134/S2070050412040150
21. Jacobsen CJH, Janssen AH, Schmidt I, Koster AJ, Jong KP (2003) Exploratory study of mesopore templating with carbon during zeolite synthesis. Microporous Mesoporous Mater 65:59–75. https://doi.org/10.1016/j.micromeso.2003.07.003
22. Narayanan S, Vijaya JJ, Sivasanker S, Yang S, Kennedy LJ (2014) Hierarchical ZSM-5 catalyst synthesized by a Triton X-100 assisted hydrothermal method. Chin J Catal 35:1892–1899. https://doi.org/10.1016/s1872-2067(14)60177-7
23. Krishnan CK, Krishnamurthy M, Kamil MSM (2016) Hierarchically structured MFI zeolite monolith prepared using agricultural waste as solid template. Microporous Mesoporous Mater 221:23–31. https://doi.org/10.1016/j.micromeso.2015.09.022
24. Jin J, Zhang X, Li Y, Li H, Wu W, Cui Y, Chen Q, Li L, Gu J, Zhao W, Shi J (2012) A simple route to synthesize mesoporous ZSM-5 templated by ammonium-modified chitosan. Chem Eur J 18:16549–16555. https://doi.org/10.1002/chem.201201614
25. Wang Y, Tao H, Li C, Ren J, Lu G (2011) Synthesis of mesoporous zeolite single crystals with cheap porogens. J Solid State Chem 184:1820–1827. https://doi.org/10.1016/j.jssc.2011.05.023
26. Xiao FS, Wang L, Yin C, Shan Z, Liu S, Du Y (2009) Bread-template synthesis of hierarchical mesoporous ZSM-5 zeolite with hydrothermally stable mesoporosity. Colloids Surf A 340:126–130. https://doi.org/10.1016/j.colsurfa.2009.03.013
27. Zhang M, Liu X, Yan Z (2016) Soluble starch as in situ template to synthesize ZSM-5 zeolite with intracrystal mesopores. Mater Lett 164:543–546. https://doi.org/10.1016/j.matlet.2015.10.044
28. Pipus G, Plazi I, Koloimi T (2000) Esterification of benzoic acid in microwave tubular flow reactor. Chem Eng J 76:239–245. https://doi.org/10.1016/s1385-8947(99)00171-0
29. Ramalinga K, Vijayalakshmi P, Kaimal TNB (2002) A mild and efficient method for esterification and transesterification catalyzed by iodine. Tetra Lett 43:879–882. https://doi.org/10.1016/s0040-4039(01)02235-3
30. Pandey AK, Singh AP (1997) A novel catalytic method for the acylation of aromatics to the corresponding ketones over zeolite catalysts. Catal Lett 44:129–133. https://doi.org/10.1023/a:1018964722746
31. Freese U, Heinrich F, Roessner F (1999) Acylation of aromatic compounds on H-Beta zeolites. Catal Today 49:237–244. https://doi.org/10.1016/s0920-5861(98)00429-5
32. Sheldon RA, Downing RS (1999) Heterogeneous catalytic transformations for environmentally friendly production. Appl Catal A 189:163–183. https://doi.org/10.1016/s0926-860x(99)00274-4
33. Treacy MMJ, Higgins JB (2001) Collection of simulated XRD powder patterns for zeolites, 4th edn. Elsevier, Amsterdam

34. Liu M, Li J, Jia W, Qin M, Wang Y, Tong K, Chen H, Zhu Z (2015) Seed-induced synthesis of hierarchical ZSM-5 nanosheets in the presence of hexadecyl trimethyl ammonium bromide. RSC Adv 5:9237–9240. https://doi.org/10.1039/c4ra14955f

35. Narayanan S, Vijaya JJ, Sivasanker S, Kennedy LJ, Jesudoss SK (2015) Structural, morphological and catalytic investigations on hierarchical ZSM-5 zeolite hexagonal cubes by surfactant assisted hydrothermal method. Powder Technol 274:338–348. https://doi.org/10.1016/j.powtec.2015.01.054

36. Maa Y, Hu J, Jia L, Li Z, Kan Q, Wu S (2013) Synthesis, characterization and catalytic activity of a novel mesoporous ZSM-5 zeolite. Mater Res Bull 48:1881–1884. https://doi.org/10.1016/j.materresbull.2013.01.014

37. Chu N, Yang J, Li C, Cui J, Zhao Q, Yin X, Lu J, Wang J (2009) An unusual hierarchical ZSM-5 microsphere with good catalytic performance in methane dehydroaromatization. Microporous Mesoporous Mater 118:169–175. https://doi.org/10.1016/j.micromeso.2008.08.048

38. Jiang J, Duanmu C, Yang Y, Gu X, Chen J (2014) Synthesis and characterization of high siliceous ZSM-5 zeolite from acid-treated palygorskite. Powder Technol 251:9–14. https://doi.org/10.1016/j.powtec.2013.10.020

39. Xue T, Wang YM, He MY (2012) Facile synthesis of nano-sized NH_4-ZSM-5 zeolites. Microporous Mesoporous Mater 156:29–35. https://doi.org/10.1016/j.micromeso.2012.02.014

40. Chu W, Yang X, Ye X, Wu Y (1996) Vapor phase esterification catalyzed by immobilized dodecatungstosilicic acid (SiW_{12}) on activated carbon. Appl Catal A 145:125–140. https://doi.org/10.1016/0926-860x(96)00109-3

41. Nandan D, Saxena SK, Viswanadham N (2014) Synthesis of hierarchical ZSM-5 using glucose as a templating precursor. Mater Chem A 2:1054–1059. https://doi.org/10.1039/c3ta13904b

42. Srivastava R, Choi M, Ryoo R (2006) Mesoporous materials with zeolite framework: remarkable effect of the hierarchical structure for retardation of catalyst deactivation. Chem Commun. https://doi.org/10.1039/b612116k

43. Silva JF, Ferracine ED, Cardoso D (2018) Effects of different variables on the formation of mesopores in Y zeolite by the action of CTA^+ surfactant. Appl Sci 8:1299. https://doi.org/10.3390/app8081299

44. Chal R, Cacciaguerra T, Donk SV, Gerardin C (2010) Pseudomorphic synthesis of mesoporous zeolite Y crystals. Chem Commun 46:7840–7842. https://doi.org/10.1039/c0cc02073g

45. Koster R, Linden BV, Poels E, Bliek A (2001) The mechanism of the gas-phase esterification of acetic acid and ethanol over MCM-41. J Catal 204:333–338. https://doi.org/10.1006/jcat.2001.3356

46. Bedard J, Chiang H, Bhan A (2012) Kinetics and mechanism of acetic acid esterification with ethanol on zeolites. J Catal 290:210–219. https://doi.org/10.1016/j.jcat.2012.03.020